Journal of Microscopy, Vol. 214, Pt 2 May 2004, pp. 174–181
Received 24 December 2003; accepted 3 February 2004

INVITED REVIEW

Evaluation of spectral imaging for plant cell analysis

R. H. BERG
Integrated Microscopy Facility, Donald Danforth Plant Science Center, 975 North Warson Road, St. Louis, MO 63132, U.S.A.

Key words. Autofluorescence, confocal microscopy, multiphoton microscopy, spectral imaging, unmixing.

Summary

Fluorescence imaging at high spectral resolution is now a practical reality and has great promise in plant cell biology. Emission spectral curve data can be used computationally to distinguish spectrally similar fluorophores, or to remove autofluorescence, and to spectrally analyse autofluorescent molecules, which are especially abundant in plant tissues. Examples of these applications in plant cells are given, and a comparison is made between the current offerings in spectral imaging laser scanning confocal microscopes.

Introduction

Spectral images differ from conventional images of optical sections by including quantitative spectral information in each pixel. This added dimension could be exploited in analysing plant cell biology, through applications in multicolour fluorescence imaging, analysis of autofluorescent molecules, and other quantitative methods such as ratio imaging and FRET. Spectral imaging detectors are available for confocal microscopes and the purpose of this paper is briefly to compare the different detectors in three confocal laser scanning microscopes and to show examples of the use of spectral imaging in plant cells. A more comprehensive review of spectral microscopy technology is given by Farkas (2001).

Conventional laser scanning microscopy images are detected using interference filters having relatively broad bandwidth, producing images with poor spectral resolution. This is often sufficient for imaging single fluorophores, and for multicomponent imaging in which the component fluorophores have adequately separated emissions. However, this limits the number of detected components to those that can be readily separated with the different filter bandwidths. Furthermore, multiphoton excitation is sometimes used to excite several fluorophores in a specimen with the same excitation wavelength, which can lead to bleed-through problems when using conventional detectors. Bleed-through problems can be minimized by means of sequential acquisition of component fluorophore signals, using fluorophore-optimized excitation (for one-photon excitation) and/or emission bandwidths. The additional time required for such acquisitions will compromise temporal resolution in studies of living cells. Plant cells are remarkable for the variety of autofluorescent molecules they can produce (Rost, 1995), and these may interfere with detection of fluorophore signal when broadband filters are used. Spectral imaging offers a means for circumventing these problems inherent with interference filter-based detection.

Spectral images typically are acquired by collecting spectral data covering emission bandwidths of the component fluorophores. Using reference spectra of the individual fluorophores present, derived from pixels in the same image or from singly stained samples run in parallel, signals of component fluorophores contained in each pixel can be 'unmixed' using simple linear equations. Fluorophores with strikingly similar emission spectra, such as fluorescein isothiocyanate (FITC) and green fluorescent protein (GFP) (peaks separated by 7 nm) can be separated computationally in an innovative approach to dealing with signal bleed-through (Dickinson *et al.*, 2001). Images comprising eight or more components are possible, limited only by the need for nominal differences in the shape of component fluorophore spectra. Autofluorescence spectra can be used as a separate component and readily separated from other signals. Indeed, the spectral imager can be used to identify autofluorescent plant molecules and study their cell biology.

To make best use of this promising technology it is important to understand its limitations and how to optimize spectral image acquisition.

Correspondence to: Dr R. Howard Berg. Tel.: +1 314 587 1261; fax: +1 314 587 1361; e-mail: rhberg@danforthcenter.org

Materials and methods

Specimens

Molecular Probes MultiSpeck beads (cat. M-7901) were used for spectral curve analysis. They were mounted in the mounting medium supplied with the beads, and the product data sheet specifies excitation/emission maxima for the blue dye are ~365/405 nm, the green dye ~520/525 nm and the red dye ~580/600 nm. Tobacco BY-2 cells were stained for unmixing with 500 nM MitoTracker Red CMXRos (Molecular Probes, cat. M-7512) in culture medium for 30 min, and then 5 μg mL^{-1} Congo Red in culture medium for 30 min, and mounted in culture medium. The tobacco BY-2 cell used for the spectral scan for Fig. 3(a) was transfected with an enhanced cyan fluorescent protein (ECFP)–HDEL construct, targeted to the endoplasmic reticulum (ER) with a leader sequence from the *Arabidopsis* chitinase gene and retained in the ER by the HDEL amino acid sequence. For Fig. 3(b), protoplasts of this same cell line were infected with tobacco mosaic virus (TMV) RNA encoding MP-EGFP, TMV movement protein fused with EGFP (Bendahmane *et al.*, 2002). The autofluorescence spectra for Fig. 4(a) are from *Arabidoposis thaliana* (Columbia ecotype) leaves (chlorophyll, cutin), root xylem elements (lignin), root endodermis (suberin) and pollen (sporopollenin). Roots of these plants were fixed for 2 h in glutaraldehyde (0.2%) or formaldehyde (4%) before measurement of autofluorescence spectra. The ECFP spectra in Fig. 4(c) were from tobacco BY-2 ER-CFP cells described above. The other fluorescent protein sources in this figure are: EGFP from MP-EGFP in TMV-infected tobacco BY-2 cells (Bendahmane *et al.*, 2002), enhanced yellow fluorescent protein (EYFP) from transgenic tobacco BY-2 cells containing EYFP-Rab GTPase, and DsRed from a transgenic tobacco BY-2 cell line with a DsRed-HDEL construct localized to the ER. The *A. thaliana* anthers in Fig. 4(d) are expressing EGFP linked to an anther wall-associated protein (Yiji Xia, Danforth Center, personal communication).

Spectral imaging

The Bio-Rad system was the Radiance 2100 Rainbow system at the Bio-Rad confocal facility in Hemel Hempstead, U.K., using an 80/30 primary beamsplitter, and using a blue diode laser (405 nm), argon laser (488 nm) and green HeNe laser (543 nm) for excitation. The Leica system was the SP2 in the Biology Department, Washington University, St. Louis. The primary beam splitter was a multichroic (488/568/632 nm), and argon (488 nm) and krypton (568 nm) lasers were used for excitation. The Zeiss META system was the Zeiss LSM 510 META NLO in the Donald Danforth Plant Science Center's (St. Louis) Integrated Microscopy Facility. Multiphoton excitation was performed using a Coherent Mira 900F Ti-sapphire tuned to 790 nm and pumped with a Verdi 10-W laser; a short-pass 650 dichroic beamsplitter was used for META spectral imaging when using multiphoton excitation. For one-photon excitation a multichroic primary beam splitter was used (UV/488/543/633 nm) with the META detector and argon (488 nm) and green HeNe (543 nm) lasers were used for excitation.

Results

Hardware compared

The three confocal microscope systems offering spectral imaging are Bio-Rad, Leica and Zeiss. Each of these has a different approach in the acquisition of a spectral image, and each can use spectral data to unmix fluorophores that suffer from bleed-through problems when acquired using conventional means.

Bio-Rad. The Bio-Rad Radiance Rainbow system uses the conventional detection channels for spectral imaging, and unmixing is based on using the fewest data points possible – as few as two to unmix two fluorophores. Emission light is split by dichroic filters, selectable from a wheel, allowing various choices in sending emission to the different PMT detectors. Unique to the Rainbow, spectral bandwidth is selected by using dual filter wheels positioned in front of each channel's PMT – there is no dispersive element in its design. These eight-position wheels, one a series of long-pass and the other short-pass filters, provides a means for selecting narrow bandwidths (~10 nm) for detection. Filter-based spectral detection provides reproducible spectral accuracy for a given PMT. In spectral scans requiring more than one PMT, the gains on these PMTs must be adjusted so that the signal in spectral transition regions between PMTs is nearly matched. If the goal is to obtain a spectrum of a fluorescent compound at high spectral resolution, then multiple acquisitions are required, each scan using a narrow bandwidth combination in the dual filter wheels of each channel, and this slow spectral acquisition could compromise spectral data if a living cell's fluorophore moves during the several minutes of acquisition (see Discussion below, Fig. 3).

By contrast, by basing unmixing on ratios between the different channels (and referring to standard ratios), a single scan may be sufficient to unmix signals. This is provided there has been appropriate selection of bandwidths and there is sufficient difference in shape of spectra in the fluorophores to be unmixed. It may be difficult to separate highly similar fluorophores (with respect to spectral curve shape) when using so few data points to describe spectral curve differences, although there is evidence that this may not be the case (Zimmerman *et al.*, 2003). It is also important to recognize that these spectral reference curves are based on intensities acquired by PMTs with separate gain settings – to use the reference curves accurately requires identical gain settings for data acquisition. The alternative is to have reference data within the experimental data image.

Signal-to-noise ratio is enhanced in this system by optimizing bandwidth for unmixing a given set of fluorophores, and given

that pinholes can be adjusted for the individual channels. A caveat of this is that when pinholes are of different diameter for each channel, data will be collected from different volumes, which will probably compromise spatial and spectral integrity between channels.

Leica. The Leica TCS SP uses the conventional detector channels to acquire data for unmixing, as in the Bio-Rad system. Spectral bandwidth is selected by combining a prism, which disperses the emission signal, with programmable slits in front of each PMT that select designated bandwidths from the dispersed spectrum. The slit apertures for PMT1 are mirrored, reflecting the wavelengths not used by PMT1 to the other PMTs. Because prism dispersal results in reduced bandwidth in the red region, relative to the blue, the slit in front of the PMT detecting red must be able to move in much smaller increments.

As in the Bio-Rad system, using only few channels for spectral detection makes for rapid data acquisition, and unmixing based on ratios from relatively few data points. Signal-to-noise ratio is also possibly high if the different fluorophores permit large bandwidth for unmixing. There is only one pinhole in the Leica system, and therefore pinhole diameter cannot be optimized for each channel. However, this does mean that there is no chance of having mismatched pinhole diameters that would gather data from different volumes in the different channels, unlike in the Bio-Rad system. As with the Bio-Rad system, if the goal is to analyse spectra at high resolution, then multiple scans are required and spectrum acquisition is a protracted process, which can be problematic in living cells (see Discussion below, Fig. 3). By contrast, spectral resolution is highest with the Leica SP, capable of single-nanometre resolution compared with 10 nm resolution in the Bio-Rad system and 10.7 nm in the Zeiss system. Higher resolution requires correspondingly higher numbers of acquisition scans.

Zeiss. The Zeiss META system uses an array of PMTs to acquire spectral information from grating-dispersed emission light. By acquiring spectra in parallel scans, acquisition of high-resolution spectral data is done in relatively short time, setting the META apart from the other two systems. The necessary compromises to this approach are that each PMT receives only (a fixed) narrow bandwidth of 10.7 nm, leading to signal-to-noise issues (e.g. all signals must fall within the dynamic range of the detector), and that only one pinhole diameter can be used for the acquisition – the PMT array is one channel in the scan head.

That there is one pinhole setting for all the spectral channels ensures all PMTs collect data from the same volume. As many as eight fluorophores can be unmixed using data acquired by a single scan, compared with four for a single scan in the other two systems. Signal-to-noise ratio can be improved by binning the PMT channels, which increases signal up to four times (binning four PMTs) at the cost of spectral resolution. This would seem to make the Zeiss system equivalent to the other two systems, with the exception that pinhole diameter cannot be changed, unlike the other systems. Grating dispersion transmission efficiency varies across the spectrum and, to compensate for this, the PMT array gain settings are factory-set to optimize signal across the spectrum. The fact that the gain settings cannot be independently adjusted for each channel by the user avoids the potential problem of having to match reference spectra channel gain settings with experimental data settings, a problem already noted for the Bio-Rad and Leica systems.

Spectral accuracy

Three-colour beads were used to compare the spectral accuracy of the three systems. Figure 1 shows spectral curves acquired using 10 nm bandwidths. The blue dye emission peak was not detected fully in the Bio-Rad system or at all in the Leica system (lack of appropriate excitation source in the particular systems used), but the spectra of the green and red fluorophores can be compared. All systems show a peak for each fluorophore within 10 nm of the bead manufacturer's specifications (green peak of 525 nm, red peak of 600 nm).

Multiple spectral measurements in the Leica SP2 (Fig. 1b), made using the 488/568/632 nm multichroic beam splitter, show with 488 nm excitation and spectral scan in PMT1 that there are two peaks, the major green peak and a smaller peak in the red region (green curve, Fig. 1b). With 568 nm excitation and spectral scan in PMT2 there are also two peaks, the major red peak and a smaller far-red peak (red curve, Fig. 1b). The two red emission peaks from the two excitation wavelengths and PMTs have differing maxima. Furthermore, a repeat measure of the green emission, using the same multichroic, excitation and PMT, shows a slightly blue-shifted maximum (yellow curve, Fig. 1b).

Multiple spectral measurements in the Zeiss META (Fig. 1c), made using either two-photon excitation or continuous wave excitation, allow comparison of the effect of two different dichroics in the beam path on measured spectra. Spectra of individually coloured or three-coloured beads show that emission peaks and curve shapes match well for these when using two-photon excitation (790 nm) and a short pass (650 nm) dichroic. Similarly, spectra of individually coloured green and red beads have the same shape and peaks of emission curves as those coloured both red and green when using the UV/488/543/633 nm multichroic beam splitter and 488 nm and 543 nm excitation. In the META, each PMT in the PMT array measures the same spectral region regardless of dichroic or excitation source. The red emission peaks from the differing excitation/dichroics are nearly identical, but the green peaks from the 488 nm excitation and the multichroic beam splitter have a maximum near 511 nm, blue-shifted relative to the 532 nm maximum from two-photon excitation and the short-pass dichroic.

The two-photon configuration for the META detector is ideal for measuring spectra without significant emission attenuation by the dichroic. This is used in Fig. 1(d) to compare the bead

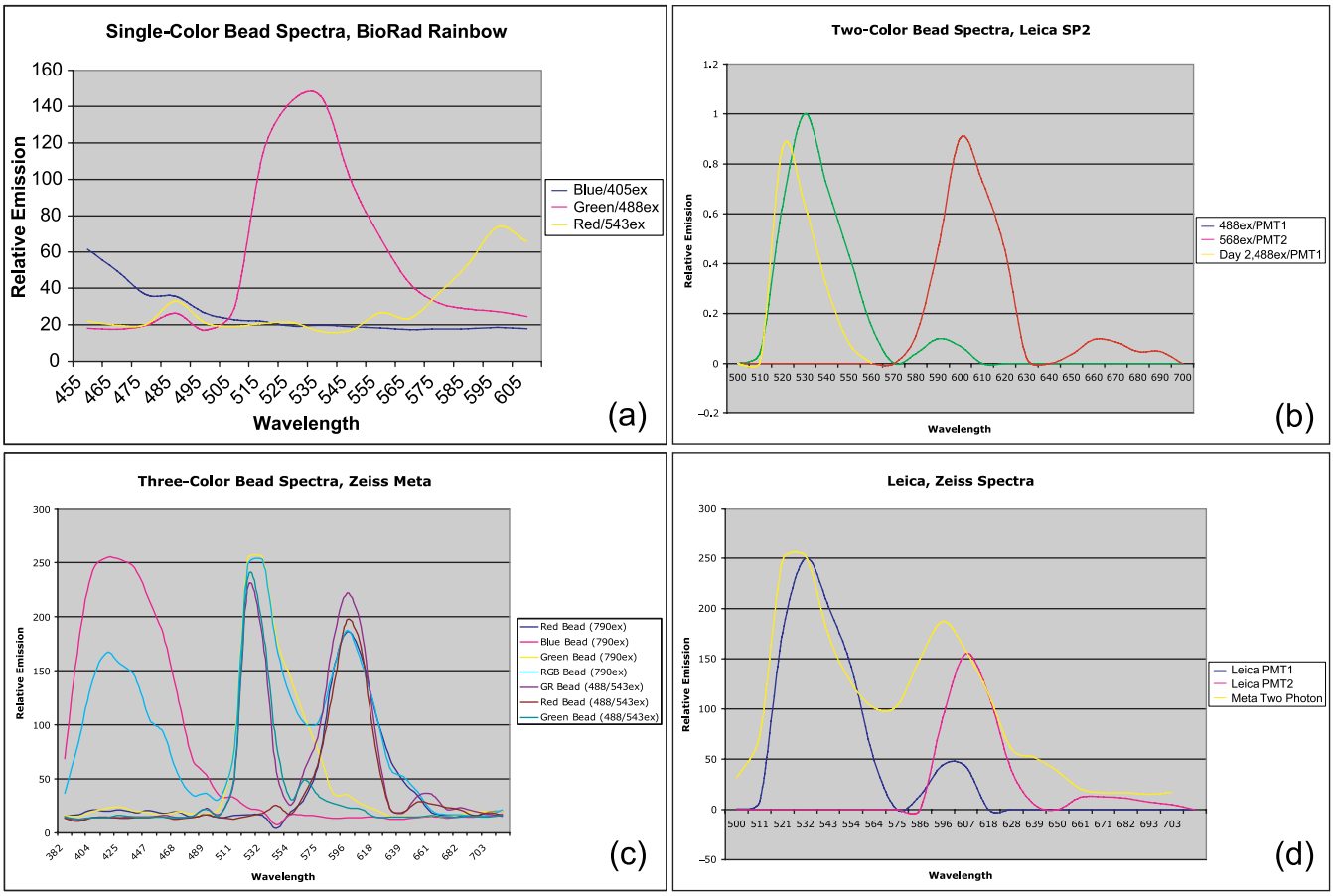

Fig. 1. Spectra of fluorescent beads acquired using spectral imagers: (a) Bio-Rad Radiance 2100 Rainbow, (b) Leica SP2, (c) Zeiss META, (d) overlay of Leica spectra and META two-photon spectra for green and red fluorophores. (a) Spectra are of singly coloured beads; (b) spectra are of two-colour beads (green, red); (c) spectra are of either singly coloured, two-coloured beads (GR = green and red), or three-coloured beads (RGB).

spectra when relatively unaffected by the (650 nm short-pass) dichroic (yellow curve) with emission attenuated by a multichroic beam splitter (blue and red curves).

Pinhole size and spectral resolution

To test the possibility that pinhole size could affect spectral resolution, spectral curves of beads were acquired using pinhole sizes ranging from 0.5 up to 4 Airy discs (data not shown). For all three systems there was negligible effect of pinhole size on spectral resolution. Bandwidth at full width half maximum (FWHM) was similar for all pinhole settings, the variation apparently more due to noise than to pinhole diameter (not correlated with disc size).

Spectral unmixing

Unmixing is a computational technique that is highly sensitive to spectral differences in the component fluorophores. Dyes with both similar emission maxima and shape of emission curve are the most challenging to unmix. Congo Red (a plant cell wall dye) and MitoTracker Red (stains mitochondria) have similar emission spectra (Fig. 2), making them good candidates for measuring a system's ability to unmix. Whether the unmix is correct can be verified by the structural location of the dyes, wall vs. mitochondrion. The unmix shown in Fig. 2 clearly shows that the Congo Red cell wall signal (green channel) is unmixed from the MitoTracker Red mitochondrial signal (red channel), using data from a single high-spectral-resolution scan on the Zeiss META.

Spectral imaging artefacts

Specimen movement. Time is of the essence: characteristic spectral shifts result if specimen movement occurs during a spectral scan. As shown in Fig. 3(a), the specimen (ER-CFP) moved up during the spectral scan, showing two images from the two scans made in the Zeiss META (inset) – the first scan (blue end of the spectrum) marked with ROI1 and plotted as the blue curve on the spectrum, the second scan (green end of the spectrum) marked with ROI2 and plotted as the pink curve on the spectrum. Averaging both scans (ROI3) gives a plot

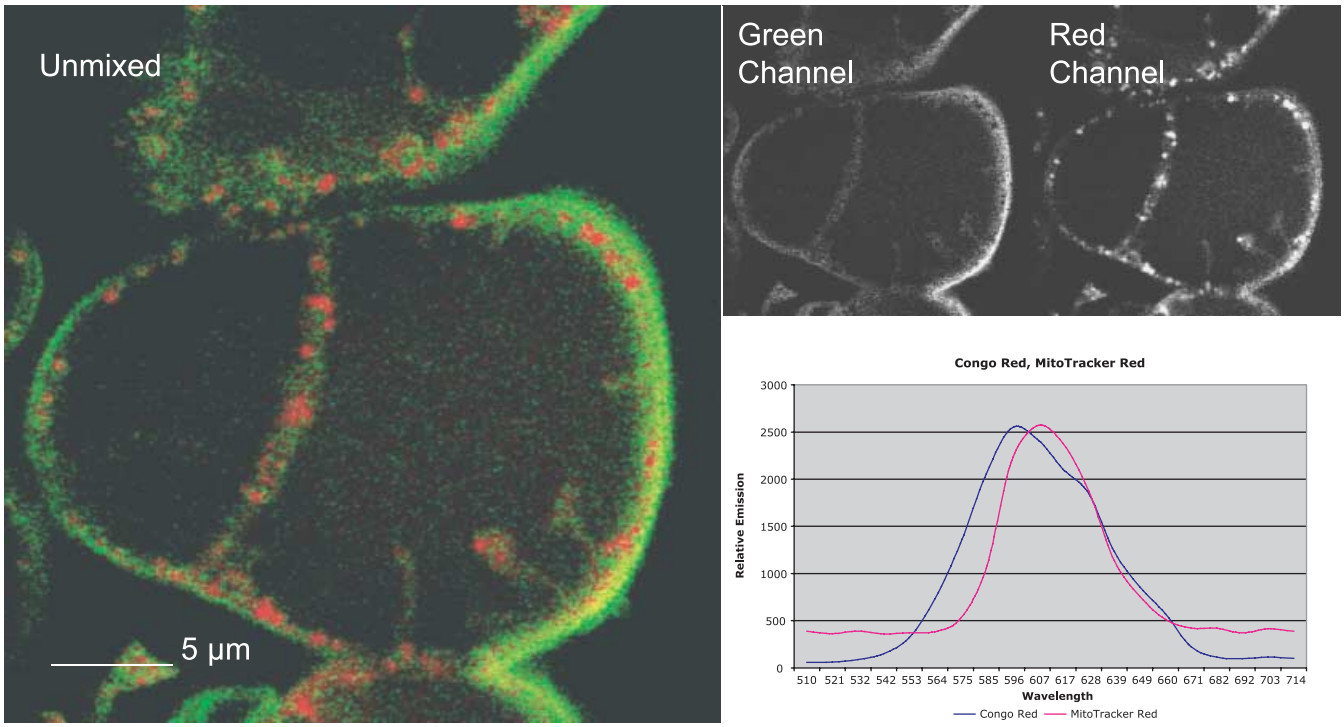

Fig. 2. Unmix of spectrally similar fluorophores in tobacco BY-2 cells stained with MitoTracker Red and Congo Red, imaged using the Zeiss META spectral imager. Reference spectra show the similarity of emission spectra; unmix was based on reference spectra contained within the same image. Mitochondria are in the red channel, cell walls in the green channel.

(yellow) that is the average of the two curves. Spectral plots of moving specimens have the characteristic sharp increase (or decrease) from baseline as seen in the pink curve.

Signal-to-noise ratio. Unmixing can only be as good as the reference spectra. Nuances of the reference spectra may have considerable influence on spectral reassignment. If the spectral scan data are too noisy, there will be errors in spectral curve shape and consequently in unmixing. The unmixed data in Fig. 3(b) indicate this dependence on noise. Shown at high magnification along the cortex of the cell, to reveal pixel colour, is a spectral unmix of ER-CFP and MP-GFP. MP is TMV movement protein, known to be in the ER in tobacco BY2 cells at this stage of infection (18 h post-infection) (Asurmendi *et al.*, 2004). Only one part of the ER in this image has enough signals from both fluorophores to give the yellow signal characteristic of co-localized signal. In the other regions the signals are too noisy, leading to errors in the unmix calculation: individual pixels were either assigned green or red colour, not yellow.

Spectra

Spectral imagers now make it relatively easy to analyse spectral features of plant cells at high temporal and spatial resolution. It should be kept in mind that these spectra are convoluted by the spectral response of the microscope, especially the beam-splitting dichroic (as discussed below). The autofluorescence emission spectra of chlorophyll and several plant cell wall components are shown in Fig. 4(a), as measured using two-photon excitation on the Zeiss META, in which case the beam-splitting dichroic (650 nm short-pass) has minimal influence on spectral curve shape (relative to dichroics used in one-photon excitation). All wall components have emission maxima in generally the same region of the spectrum, but only the curve shape of the pollen wall component sporopollenin is relatively simple. The related wall polymers suberin, cutin and lignin have remarkably similar and complex emission curve shapes. Glutaraldehyde has a bright, broad signal when it is cross-linked in tissue (Fig. 4b), and the emission of formaldehyde is weak, reflecting its poor cross-linking/retention when used as a fixative (Fox *et al.*, 1985). Fluorescent proteins measured in plant cells (Fig. 4c) have emission curves nominally similar to those published by others (Patterson *et al.*, 2001), except for ECFP, which displays the various emission curves shown. Sporopollenin (Fig. 4a, dark blue curve, ~500 nm emission maximum) and EGFP (Fig. 4C, green curve, ~511 nm maximum) have similar peaks and shapes to their emission curves, making them a challenge for spectral unmixing. They are unmixed in Fig. 4(d), using high-resolution spectral scans from the Zeiss META. Sporopollenin is in the pollen wall and also in the tapetum (T); the anther-wall-associated EGFP construct is in

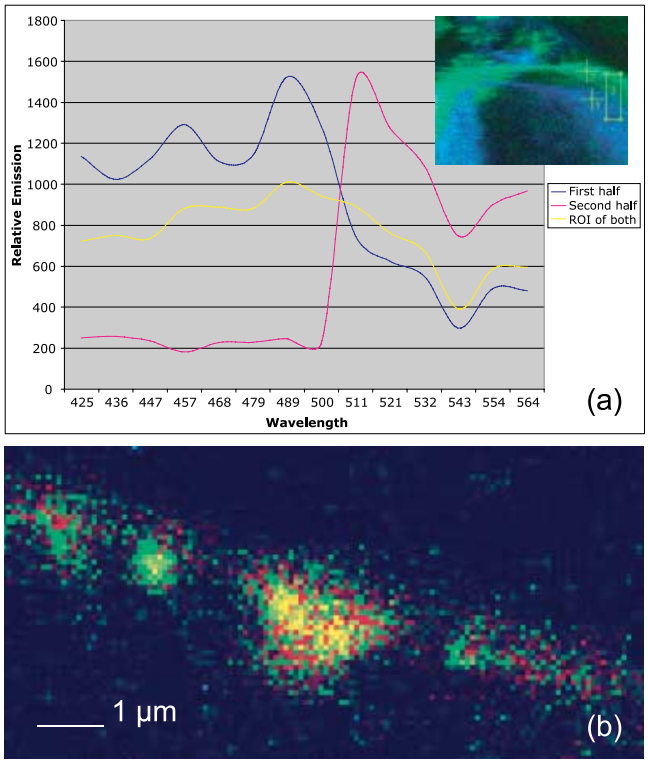

Fig. 3. Effect on spectral images of specimen movement (a) and noise (b). Imaged using the Zeiss META. (a) During spectral scan the ER-ECFP signal moved, producing a double image of the signal (inset). The first of two scans producing a blue image (ROI 1, inset) having the indicated spectrum, and the second scan producing a green image (ROI 2, inset) having the indicated spectrum. ROI 3 averages the two signals. (b) Enlarged view of the cortex of a tobacco BY-2 cell expressing ER-ECFP and MP-EGFP, co-localized in the cortical ER. This is an unmixed image and image noise prevents adequate unmixing except in the brightest region, where yellow indicates the co-localized signal.

the tapetum (co-localizing in yellow with sporopollenin) and in outer cells of the anther wall.

Discussion

There are a number of applications for spectral imaging. Spectra can be used to unmix fluorophores, computationally identifying their two-dimensional distribution when interference filters are unable to do so. Overlapping fluorescence emissions of fluorophores can be identified via their spectra, to aid in selection of appropriate bandpass filters for conventional imaging, and to optimize separation by sequential acquisition. Detailed spectral profiles of indigenous or introduced fluorophores have the potential to reveal functional information about cellular processes. Subtle changes in emission curves detected over time have applications that include photoconversion (such as with the Kaede proteins), FRET analysis and dye ratio imaging. Spectral images simply enhance our ability to understand and interpret fluorescence images.

Unmixing

Unmixing has stimulated much interest in spectral imaging (Lansford *et al.*, 2001; Bezanilla *et al.*, 2003; Zimmerman *et al.*, 2003). Of the systems compared in this paper, data acquisition for unmixing is performed in two ways. The Bio-Rad and Leica systems use bandpass filters (Bio-Rad) or prism spectrometer (Leica) to acquire the minimum data required for unmixing (number of channels = number of fluorophores), using separately acquired spectral data to identify the optimal bandpasses for distinguishing the fluorophores. This has been shown to allow unmixing of EGFP and YFP (Zimmerman *et al.*, 2003), which suffer from bleed-through due to their similar emissions (Fig. 4c). Unmixing of fluorophores with nearly identical emissions requires enough data to identify their spectral differences. To do this in one pass, the Bio-Rad and Leica systems must do this with at most four data points, from up to four detectors. The Zeiss META's scan of PMTs in parallel, by contrast, can acquire eight data points in one scan of an ~85 nm band. The unmix of nearly identical fluorophores in Figs 2 and 4(d) is based on high-resolution spectral data that can be acquired in two scans on the Zeiss META. The META has been used to unmix a variety of GFP variants, and GFP and FITC (Lansford *et al.*, 2001). It has been used to unmix DsRed from GFP in plants (Bezanilla *et al.*, 2003) and DsRed from chlorophyll (Berg *et al.*, 2002). The two approaches to unmixing have their different benefits: the minimal data approach of Bio-Rad and Leica allows rapid spectral data acquisitions; the maximum data approach of Zeiss META produces more spectral resolution per scan period. The Bio-Rad and Leica systems can unmix up to four components. In a significant difference, the META can unmix up to eight components. The Zeiss system can also use the multichannel/minimum data approach in the most recent version of system software.

There is the issue of noise. Individual PMTs in the Zeiss META array receive only 10.7 nm bandwidth in high-resolution scans, requiring steps to improve signal-to-noise ratio for dim signals. The array gives high spectral resolution in minimum number of scans, but these data are only useful if they are significantly above the shot noise. By contrast, in the Bio-Rad and Leica systems, reference spectra stored for later use in unmixing have 'shape' due in part to the relative gain settings on the different PMTs used to detect them. The shape of spectra in experimental samples also is affected by the relative gain settings in the different PMTs used in their acquisition. To unmix accurately the experimental data using stored reference spectra it is important to use the same PMT gain settings for the two data sets.

For live cell imaging, in which specimen movement can be a problem (Fig. 3a), rapid spectral scans are desirable and all three systems can do this when acquiring data for unmixing. The Zeiss META has the option of acquiring high spectral resolution in a single scan (covering ~85 nm), for use in unmixing highly similar fluorophores or in analysing spectra profiles dynamically.

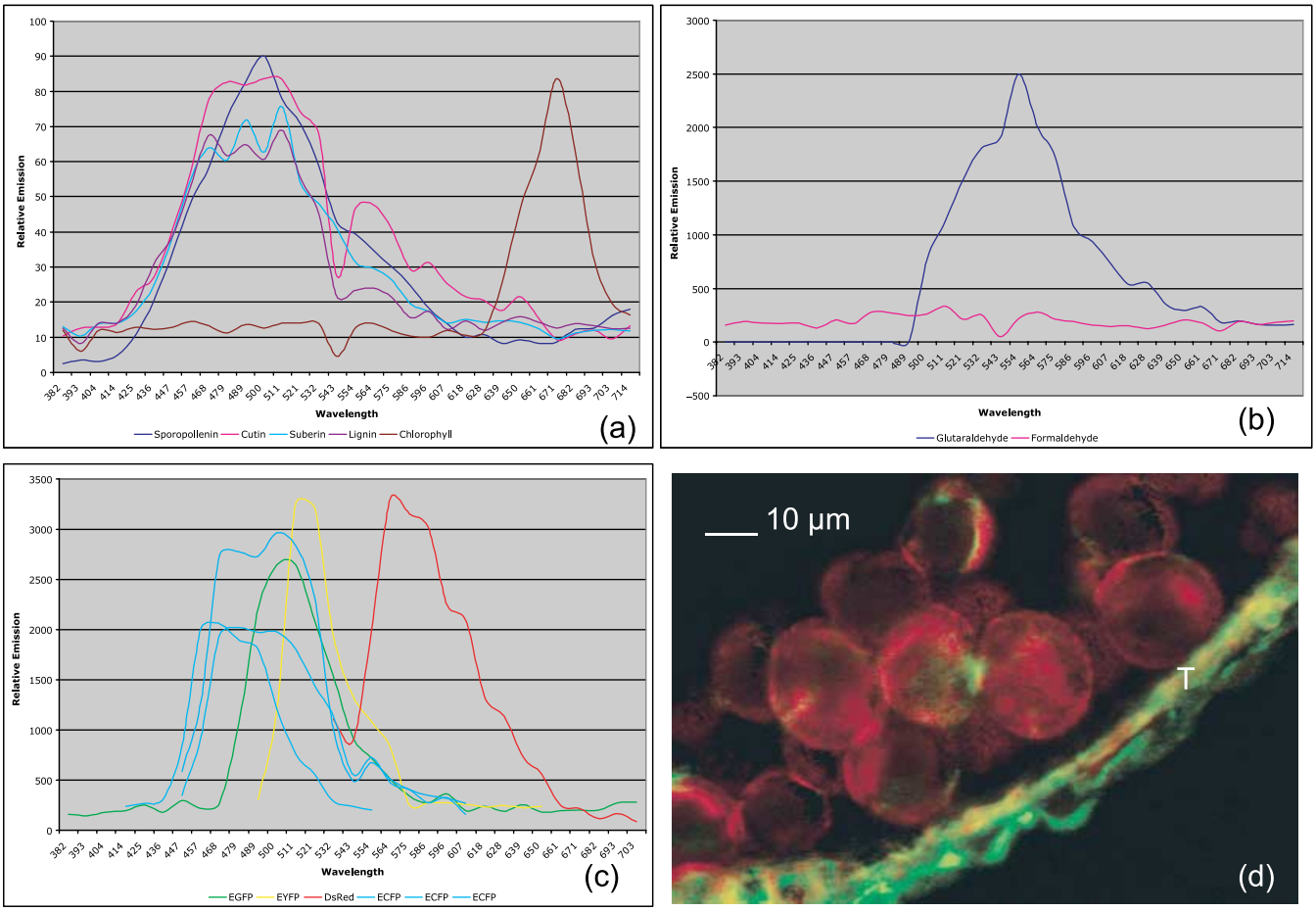

Fig. 4. Spectral profiles of fluorescent molecules in *Arabidopsis*, using the Zeiss META. (a) Autofluorescence of plant wall polymers and chlorophyll. (b) Autofluorescence introduced by fixatives. (c) Fluorescent proteins (constructs described in Methods). (d) Unmix of spectrally similar sporopollenin and EGFP in anther tissue (T, tapetum).

Spectral profiling

Autofluorescent molecules are abundant in plant cells (Rost, 1995) and spectral imagers offer a means for analysing their spectra, yielding information on their development and function. All three systems can acquire high-resolution spectra. Because the Zeiss META scans spectra in parallel, and the Bio-Rad Rainbow and Leica SP scan in series, there is a huge difference in the amount of time required for acquiring high-resolution spectra. The Zeiss covers the entire visible region in four scans, whereas the other two systems require dozens of scans to cover this region – a potential problem for moving objects in living cells and for photobleaching the sample.

Spectral imagers are not unbiased spectrometers. All optical components of the microscope and spectral imaging system affect the shape of acquired spectra, complicating interpretation of nuances in spectral curves, as shown in Fig. 4. Even emission maxima can be affected, as is evident in Fig. 1(b–d). The emission curve resulting from 488 nm excitation in Fig. 1(b) produces a maximum for the red fluorophore that is significantly blue-shifted relative to the peak resulting from 568 nm excitation. This is probably not due to the differing excitation wavelengths; according to Kasha's rule (Lakowicz, 1999) the same emission curve usually results when different excitation wavelengths are used. Rather, it appears to be an effect of the primary multichroic beam splitter. Beam-splitter multichroics have been shown to subtly affect spectral emission due to transmission bandwidth restrictions in the beam-splitter (Seyfried *et al.*, 2003). Earlier versions of the Leica SP used multiband dichroics to reflect excitation wavelengths; current versions use an acousto-optical filter (AOBS). The Leica bead spectra shown here are derived from a system with the multi-dichroic beam splitter, with transmission dips at 568 nm and 633 nm. According to the bead manufacturer, the red bead fluorophore is not excited by 488 nm, meaning the second peak attributed to excitation by 488 nm and emission by the red fluorophore in Fig. 1(b) is actually the trailing slope of emission by the green fluorophore, the dip caused by the dip in transmission of the multichroic beam splitter. This is supported by the emission data in Fig. 1(d). The yellow curve

is emission from a two-colour bead excited by two-photon absorption of 790 nm light, detected on the Zeiss META without mutichroic beam splitter in the light path and therefore showing more of the shape of the emission curves. Overlaid on this are two of the curves from Fig. 1(b), showing that the emission dip for the red fluorophore by the multichroic causes an apparent red-shift in emission maximum in addition to an artefactual second peak from the green fluorophore. The apparent peak in the far red is also the trailing slope from the red fluorophore that shows a dip due to the 633 reflection band on the multichroic. Similarly, the multichroic beam-splitter in the Zeiss META causes a blue-shifted green fluorophore peak when 488 excitation is used (Fig. 1c, green emission curves with 488 nm excitation). For the Zeiss META, two-photon excitation is ideal for spectral imaging because of the elimination of the beam-splitter effect and the common ability to excite multiple fluorophores with one excitation line and then use unmixing to correct for bleed-through.

Acknowledgements

I would like to thank Bio-Rad, Hemel Hempstead, U.K., for giving access to the Radiance 2100 Rainbow spectral imager, and Mike Veith of the Biology Department, Washington University, St. Louis, for providing access to the Leica SP2, and to the NSF Major Research Instrumentation program, for funding a grant awarded to the Danforth Center Integrated Microscopy Facility, to purchase the Zeiss META system. I am grateful to Chris Power (Bio-Rad), Volker Seyfried (Leica) and Sebastian Tille (Zeiss) for fielding my questions on their spectral imaging systems. I express my appreciation to Masaaki Fujiki, Yiji Xia, Charles Dietrich and Erik Nielsen of the Danforth Center for contributing specimens containing fluorescent protein constructs.

References

Asurmendi, S., Berg, R.H., Koo, J.C. & Beachy, R.N. (2004) Coat protein regulates formation of replication complexes during TMV infection. *Proc. Natl Acad. Sci. USA*, **101**, 1415–1420.

Bendahmane, M., Szecsi, J., Chen, I., Berg, R.H. & Beachy, R.N. (2002) Characterization of mutant tobacco mosaic virus coat protein that interferes with virus cell-to-cell movement. *Proc. Natl Acad. Sci. USA*, **99**, 3645–3650.

Berg, R.H., Asurmendi, S. & Beachy, R.N. (2002) TMV infection cycle in plant cells revealed by 3-D microscopy. *Microsc. Microanal.* **8** (Suppl. 2), 966CD.

Bezanilla, M., Pan, A. & Quatrano, R. (2003) RNA interference in the moss *Physcomitrella patens*. *Plant Physiol.* **133**, 470–474.

Dickinson, M.E., Bearman, G., Tille, S., Lansford, R. & Fraser, S.E. (2001) Multi-spectral imaging and linear unmixing add a whole new dimension to laser scanning fluorescence microscopy. *Biotechniques*, **31**, 1272–1278.

Farkas, D.L. (2001) Spectral microscopy for quantitative cell and tissue imaging. *Methods in Cellular Imaging* (ed. by A. Periasamy), pp. 345–363. Oxford University Press, New York.

Fox, C.H., Johnson, F.B., Whiting, J. & Roller, P.P. (1985) Formaldehyde fixation. *J. Histochem. Cytochem.* **33**, 845–853.

Lakowicz, Joseph, R. (1999) *Principles of Fluorescence Spectroscopy*. Kluwer Academic/Plenum Publishers, New York.

Lansford, R., Bearman, G. & Fraser, S.E. (2001) Resolution of multiple green fluorescent protein color variants and dyes using two-photon microscopy and imaging spectroscopy. *J. Biomed. Optics*, **6**, 311–318.

Patterson, G., Day, R.N. & Piston, D. (2001) Fluorescent protein spectra. *J. Cell Sci.* **114**, 837–838.

Rost, F.W.D. (1995) Autofluorescence in plants, fungi and bacteria. *Fluorescence Microscopy*, Vol. II (ed. by F. W. D. Rost), pp. 16–39. Cambridge University Press, New York.

Seyfried, V., Birk, H., Storz, R. & Ulrich, H. (2003) Advances in multispectral confocal imaging. *Proc. SPIE*, **5139**, 147–157.

Zimmerman, T., Rietdorf, J. & Pepperkok, R. (2003) Spectral imaging and its applications in live cell microscopy. *FEBS Lett.* **546**, 87–92.